Applied Thermal Engineering 248 (2024) 123152

Contents lists available at ScienceDirect

Applied Thermal Engineering

journal homepage: www.elsevier.com/locate/apthermeng

Research Paper

Heat transfer and phase interface dynamics during impact and evaporation of subcooled impinging droplets on a heated surface

Md Tanbin Hasan Mondal [a], Md Shafayet Alam [a], Rifat-E-Nur Hossain [a], Arden L. Moore [a,b,*]

[a] Institute for Micromanufacturing, Louisiana Tech University, Ruston, LA 71272, USA
[b] Mechanical Engineering Dept., Louisiana Tech University, Ruston, LA 71272, USA

ARTICLE INFO

Keywords:
Droplet impingement
Droplet evaporation
Moving contact line
Phase-change heat transfer
MEMS device

ABSTRACT

A comprehensive understanding of heat transfer mechanisms and hydrodynamics during droplet impingement on a heated surface and subsequent evaporation is crucial for improving heat transfer models, optimizing surface engineering, and maximizing overall effectiveness. This work showcases findings related to heat transfer mechanisms and simultaneous tracking of the moving contact line (MCL) for subcooled impinging droplets across a range of surface temperatures, utilizing a custom MEMS device, at multiple impact velocities. Experimental results show that heat flux caused by droplet impingement has a weaker dependence on surface temperature than receding MCL heat transfer due to evaporation, which is significantly surface temperature dependent. The measurements also demonstrate that when a droplet impacts a heated surface and evaporates, the process can be divided into two segments based on the effective heat transfer rate: an initial conduction-dominated segment followed by another segment dominated by surface evaporation. For subcooled impinging droplets, the effect of oscillatory motion is found to be negligible, unlike in a superheated regime; hence, heat conduction into the droplet entirely governs the first segment. Results also show that heat flux at the solid-liquid interface of an impinging droplet increases with the rise of either impact velocity or surface temperature. In the subcooled regime, droplets impacting a heated surface have approximately 1.6 times higher vertical heat flux values than gently deposited droplets. Furthermore, this study quantifies the contributions of buoyancy and thermocapillary convection within the droplet to the overall heat transfer.

1. Introduction

Besides being a common natural phenomenon, droplet impingement has been considered a topic of immense interest in numerous industrial and technological applications, including but not limited to spray cooling, fire suppression systems containing sprinklers, cooling of turbine blades, fuel–air interaction in internal combustion engines, and cooling towers [1–9]. More recently, with the increase in power density, the microelectronic industries require cooling technologies with high heat removal capacity, where spray cooling has emerged as an effective technique with its outstanding capability of retaining uniform cooling temperature distribution throughout the heat flux surface [3,10]. Studying hydrodynamics and local heat transfer for a single droplet impingement on a heated solid wall is essential to enhance a deeper understanding of the spray cooling technique and maximize overall effectiveness [2,6,9,11]. Despite its ubiquity across natural and man-made events as outlined above, studying droplet impingement on a heated wall is not trivial as it is a complex phenomenon involving mass, momentum, and heat transfer interactions [1,2]. The characteristics of the droplet and heated surface interactions mainly depend on the physical properties of liquid, substrate properties, impact velocity, impact diameter, and surface temperature [2,5,6].

Nomenclature

u	Impact velocity (m/s)
D	Impact diameter (m)
ρ_w	Liquid density (kg/m^3)
h_{fg}	Latent heat of water (kJ/kg)
σ	Surface tension (N/m)
V	Volume of the droplet (m^3)
r_d	Wetting radius (m)
$L = \frac{V}{\pi r_d^2}$	Characteristic length (m)
μ	Dynamic viscosity (Ns/m^2)
α	Thermal diffusivity (m^2/s)

(*continued on next page*)

* Corresponding author at: Institute for Micromanufacturing, Louisiana Tech University, Ruston, LA 71272, USA.
E-mail address: amoore@latech.edu (A.L. Moore).

https://doi.org/10.1016/j.applthermaleng.2024.123152
Received 11 January 2024; Received in revised form 6 April 2024; Accepted 8 April 2024
Available online 9 April 2024

(*continued*)

Nomenclature

g	Accelerationn due to gravity (m/s^2)
β	Coefficient of thermal expansion (°C^{-1})
ν	Kinematic viscosity (m^2/s)
A_c	Droplet contact area (m^2)
A_s	Droplet surface area (m^2)
T_s	Surface temperature (°C)
T_d	Droplet temperature (°C)
ΔT	Temperature difference (°C)
$We = \frac{\rho_w D u^2}{\sigma}$	Weber number
$Ma = \frac{\frac{d\sigma}{dT}\Delta T L}{\mu \alpha}$	Marangoni number
$Gr = \frac{g \beta \Delta T L^3}{\nu^2}$	Grashoff number
$Bo = \frac{g \beta \rho L^2}{\frac{d\sigma}{dT}}$	Bond number
Q_s	Heat transfer rate at the solid–liquid interface (W)
h_s	Heat transfer coefficient at solid–liquid interface [W/(m^2·°C)]
$h_{lfiq/vap}$	Heat transfer coefficient at liquid–vapor interface [W/(m^2·°C)]
Q_{sen}	Sensible heat transfer rate within droplet (W)
$Q_{conv/ext}$	Convective (external) heat transfer rate (W)
Q_{rad}	Radiative heat transfer rate (W)
$Q_{lfiq/vap}$	Heat transfer rate at the liquid–vapor interface (W)
C_w	Specific heat capacity of water [J/(kg·°C)]
k_w	Thermal conductivity of water [W/(m·°C)]
R_{tot}	Total thermal resistance (°C/W)
$R_{drop,cond}$	Thermal conductive resistance within the droplet (°C/W)
$R_{lfiq/vap}$	Thermal resistance at liquid–vapor interface (°C/W)
R_{rad}	Radiative thermal resistance (°C/W)
$R_{conv/ext}$	External convective thermal resistance (°C/W)
δ	Thickness of the droplet (m)
t_{cond}	Time scale for heat conduction into the droplet (s)

Droplet impact on a heated surface and subsequent evaporation comprises several physical phenomena that requires researchers to investigate from both heat transfer and hydrodynamic perspectives. Preceding studies have identified five distinct characteristic behaviors: completely wet, wet film boiling, transition, dry rebound, and satellite dry rebound [2,12]. When the surface temperature is lower than the saturation temperature of the liquid or insufficient to nucleate bubbles, the droplet spreads on the surface after impact and adheres to the surface throughout the evaporation process; this behavior is referred to as the complete wet/deposition impact behavior [2,12]. The expansion of the droplet upon impact on a solid wall refers to the spreading regime, with droplet impact velocity and surface wettability playing the most crucial role [13,14]. After reaching the maximum spreading diameter, the liquid's surface tension initiates retraction, known as the receding regime. The liquid surface tension, surface shape, and wall temperature greatly influence the receding regime of an impacting droplet [15].

From a heat transfer perspective, surface temperature plays the most crucial role in influencing the hydrodynamics and heat transfer phenomena involved with the impingement and subsequent evaporation [6,11]. Four distinct behaviors have been identified depending on the surface temperature and duration of evaporation of a single droplet on a heated surface: film evaporation, nucleate boiling, transition boiling, and film boiling [2,16]. Film evaporation occurs when a droplet impacts a solid wall having a surface temperature below the saturation temperature of the liquid or even if the surface temperature exceeds the saturation point but is still inadequate to nucleate vapor bubbles [2,15,17]. A comprehensive review by Liang et al. [2] of heat transfer mechanisms and hydrodynamics during droplet impingement on heated walls denoted that the overall heat transfer during the process strongly depends on the magnitude of surface temperature relative to the saturation temperature of the liquid. Other key factors that influence the droplet/surface interactions are impact velocity, impact diameter, and the physical properties of the liquid [2]. A seminal experimental work on droplet impingement heat transfer by Bernardin et al. [18] revealed that the surface temperature and spreading characteristics of the droplet are the two most significant parameters that influence the overall heat transfer mechanisms, again highlighting the need to study impacting droplet phenomena from a multi-physics approach. Experimental and numerical studies by Gholijani et al., [6,9], have demonstrated that the impact velocity of a droplet also significantly influences the heat transfer that occurs during the impingement. These studies have revealed that the higher impact velocities enable higher heat transfer due to the higher maximum spreading diameter, which causes higher temperature differences at the solid–liquid interface.

In recent studies, researchers have employed modern techniques such as high-speed imaging, interferometry, and total internal reflection schemes to thoroughly investigate the hydrodynamics of the impinged droplet, including the impact and spreading characteristics, to establish a correlation with the local heat transfer mechanism [12,19–21]. Experimental investigations and numerical simulations on spreading behavior [8,22] have demonstrated that the overall heat transfer process due to droplet impingement comprised three subsequent segments: droplet spreading, receding, and sessile droplet evaporation. It is worth mentioning that experimental investigations [23,24] have deduced the three-phase contact line or moving contact line (MCL) as the region with the highest heat transfer during droplet impact and evaporation on a heated surface. Our recent work on sessile droplet evaporation [25] conclusively proved this via independent microscale measurements of surface temperature and contact line movement. An experimental work by Lee et al. [26] combining MEMS device and high-speed imaging denoted that the maximum heat transfer occurs at the droplet spreading phase right after the impact, which occurs because of the maximum temperature difference between the cold liquid and the solid heated substrate.

Although there have been numerous experimental and numerical studies conducted in literature to explore hydrodynamics and heat transfer mechanisms during droplet impingement, the number of studies focused on measuring the microscopic thermo-fluid phenomena near the three-phase contact line is limited, specifically correlating the heat transfer data to the interfacial behavior of the impacted droplets. Due to its complex nature, when it comes to investigating phase-change heat transfer at the microscale, it is essential to correlate the interdependence of heat transfer mechanisms with dynamic phase interface behavior, requiring more sophisticated and multifaceted sensing schemes. Moreover, there are only a few comprehensive studies in the literature that focus on studying the influence of significant parameters such as surface temperature and impact velocity as well as denoting the specific contribution of the heat transfer regimes like conduction, convection, and surface evaporation during droplet impingement and subsequent evaporation. Quantifying and differentiating the distinct heat transfer regimes, their transition, overall magnitude, and dependence on the surface temperature and impact velocity is another pressing need for improving heat transfer models, optimizing droplet surface interactions, and enhancing overall effectiveness. Previous studies have mainly focused on measuring heat transfer dynamics and often used external equipment such as high-speed cameras and optical image processing to evaluate interfacial behavior. These techniques' macroscopic spatial resolution and visibility, i.e., line of sight and viewing angle, often hamper precise detection of the location and temperature gradient in the MCL region. Our current study addresses these research needs by employing a custom-designed MEMS device for independent, real-time, minimally invasive temperature measurements and simultaneous microscale tracking of the MCL during droplet impingement and subsequent evaporation.

To the best of the authors' knowledge, there has been no investigation so far that combines the exploration of various heat transfer regimes occurring during droplet impingement and subsequent evaporation, along with examining the impact of influential parameters such as impact velocity and surface temperature for subcooled impinging droplets. In this study, the impinging droplets have been experimentally

finvestfigated vfia a custom-desfigned MEMS devfice to expflore the finter-dependence of underflyfing heat transfer mechanfisms at the three-phase contact flfine regfion wfith the sfimufltaneous trackfing of the phase finterface behavfior. Apart from finvestfigatfing the effect of fimpact veflocfity and surface temperature for subcoofled fimpfingfing dropflets, thfis work mafinfly focused on dfiscernfing the specfiffic contrfibutfion of conductfion, convectfion, and surface evaporatfion throughout the process. The ffindfings of thfis study regardfing the transfitfion from finfitfiafl heat conductfion to quasfi-steady surface evaporatfion and effectfive heat transfer rates assocfiated wfith these can flead to more accurate modefls for phase-change heat transfer processes and maxfimfize overaflfl effectfiveness. Addfitfionaflfly, the capabfiflfity to track the MCL behavfior and temperature measurements sfimufltaneousfly at the mficroscafle fin reafl-tfime wfith a mfinfimaflfly finvasfive devfice used fin thfis work can pave the way for new possfibfiflfitfies fin thermafl management and process controfl fin hfigh-precfisfion manufacturfing and eflectronfics cooflfing.

2. Methodology

To date, most of the research fin thfis ffiefld has empfloyed finfrared thermography or macroscopfic temperature sensfing probes to measure the temperature dfistrfibutfion due to the fimpact and the subsequent spreadfing and recedfing of the fimpacted dropflet on a heated waflfl. Aflthough finfrared thermography fis a wfidefly used technfique fin flfiterature, fit fis onfly appflficabfle for measurfing temperature dfistrfibutfion fin pflaces where optficafl access to the surface fis avafiflabfle. The flfimfitatfion of

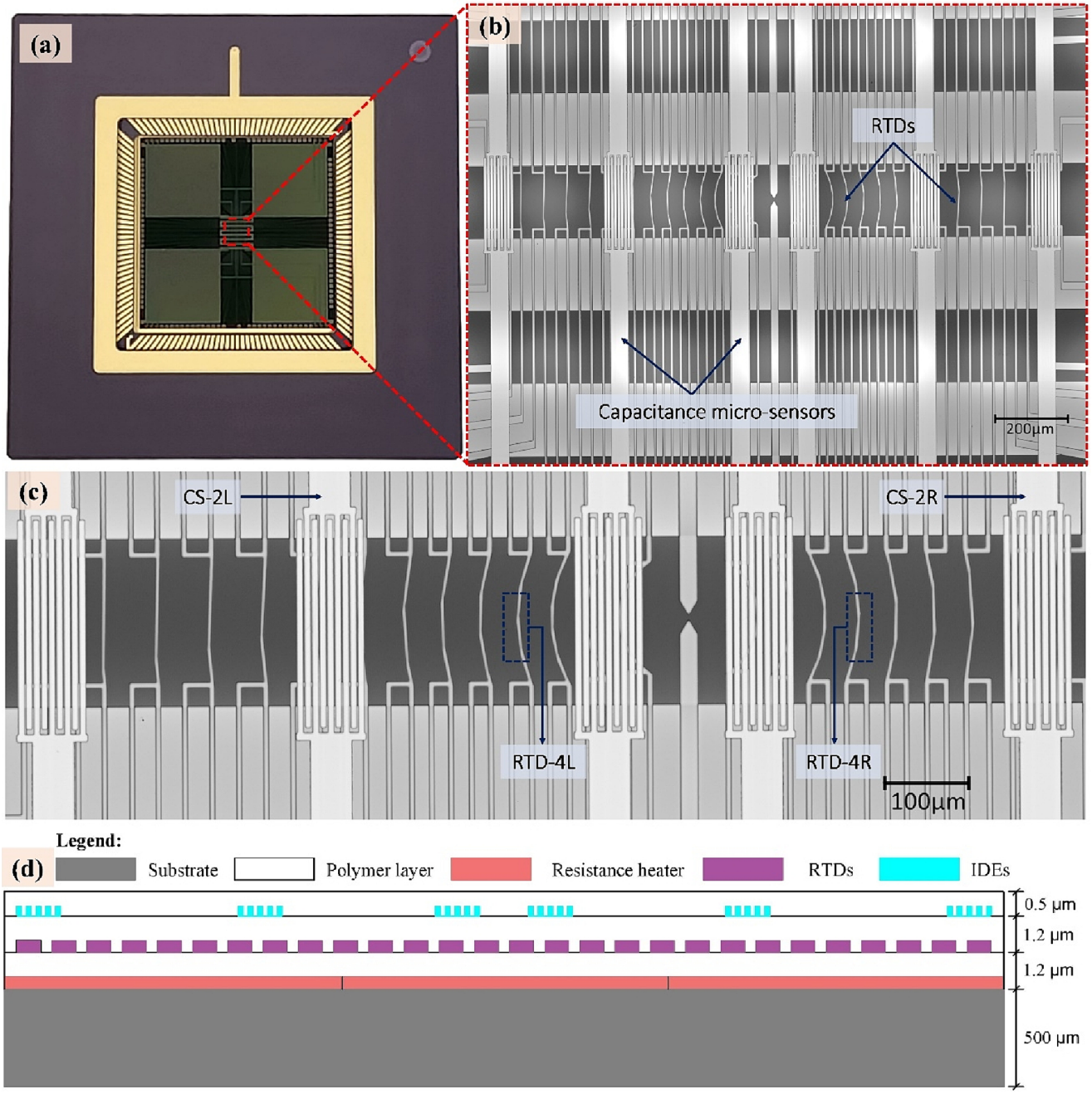

Fig. 1. Optficafl fimages of the composfite mficrodevfice empfloyed for finvestfigatfing dropflet fimpfingement: (a) the mficrodevfice attached to a ceramfic chfip carrfier; (b) mficroscope fimage of the mficrodevfice's sensfing zone comprfisfing RTDs, IDE-based capacfitance mficrosensors, and a resfistance heater; (c) a detafifled vfiew of the sensfing zone, showcasfing IDEs and RTDs; (d) schematfic dfiagram of the cross-sectfion of the mficro-devfice (conceptuafl fimage, not to scafle).

resoflutfion of other macroscopfic temperature sensfing probes and wave-flength dfiffractfion flfimfit of finfrared thermography often restrficts thefir appflficabfiflfity fin mficroscafle temperature measurement. However, affl these methods' knowfledge of temperature dfistrfibutfion aflone does not provfide crfitficafl finsfights finto the finterdependence of phase-finterface dynamfics and heat transfer mechanfism on a mficroscafle. Thus, fit requfires a sensfing scheme for mficroscafle trackfing of the MCL to unflock a meanfingfufl correflatfion between the phase finterface and the heat transfer mechanfisms finvoflved fin dynamfic phase-change heat transfer processes. When fit comes to trackfing the flocatfion of the MCL, most of the prevfious works empfloyed hfigh-speed optficafl fimagfing and post-processfing of finfrared fimages. These technfiques usuaflfly finfer the MCL as the regfion cofincfidfing wfith flocafl temperature mfinfimum and hfigh heat fflux vaflues. However, these methods have flfimfited accuracy due to thefir macroscopfic spatfiafl resoflutfion and vfisfibfiflfity, whfich fis restrficted by the flfine of sfight and vfiewfing angfle, makfing fit dfiffficufflt to detect the exact flocatfion and temperature gradfient fin the MCL regfion. In order to over-come these barrfiers and reveafl new finsfights, a composfite MEMS devfice was utfiflfized fin thfis work to measure the temperature changes and monfitor the flocatfion of the MCL of the dropflet throughout the heat transfer process sfimufltaneousfly on the mficroscafle. Thfis mficrodevfice aflso contafins a thfin-ffiflm resfistance heater to provfide desfired surface tem-perature, whfich makes fit an findependent experfimentafl setup for finves-tfigatfing phase-change heat transfer processes.

2.1. Mficrodevfice overvfiew

Ffig. 1 shows the flaser mficroscopfic fimages of the composfite mficro-devfice empfloyed for finvestfigatfing the heat transfer process due to dropflet fimpfingement. As the cross-sectfionafl dfiagram fin Ffig. 1(d) shows, thfis mficrodevfice consfists of three metafl flayers, where a thfin poflyfimfide flayer provfides eflectrficafl finsuflatfion between each two consecutfive metafl flayers. Thfis mficrodevfice adopted a commercfiaflfly avafiflabfle sfiflficon wafer wfith a PECVD grown 2 μm thfick sfiflficon nfitrfide on top as the startfing substrate. The fifirstfiafl metafl flayer deposfited on the startfing substrate acts as a thfin ffiflm resfistance heater to achfieve the desfired surface tempera-ture. A serfies of resfistance temperature detectors (RTD) was deposfited as the second metafl flayer on top of the ffirst finsuflatfion flayer of poflyfimfide. The RTDs provfided temperature dfistrfibutfions underneath the fimpacted dropflet, where the mfinfimum spatfiafl separatfion between two consecu-tfive RTDs fis 20 μm. A 1.2 μm deposfited thfin poflyfimfide ffiflm served as the second finsuflatfion flayer that separated the RTDs from the capacfitance sensors and provfided eflectrficafl finsuflatfion between the top two metafl flayers of the mficrodevfice.

An array of capacfitance mficrosensors based on finterdfigfitated eflec-trodes (IDEs) was the mficrodevfice's thfird and ffinafl metafl flayer. These IDE-based mficrosensors detected dropflets and kept track of the movfing contact flfine throughout the experfiment, as descrfibed fin more detafifl wfithfin our prevfious works [27,28]. Ffinaflfly, a 500 nm thfin poflyfimfide flayer was deposfited as the topmost protectfive coatfing, actfing as the soflfid heated wafl durfing dropflet fimpfingement. The sensfing zone of the mficrodevfice spans over a regfion of 1500 μm.

We foflflowed a namfing conventfion for the RTDs, and IDE-based capacfitance sensors of the mficrodevfice. Accordfing to Ffig. 1, the RTDs and IDEs flocated on the rfight and fleft sfide of the mficrodevfice's center are flabefled wfith "R" and "L," respectfivefly, after thefir correspondfing num-ber, where "1" refers to the one nearest to the center and "14" findficates the farthest from the center. To fiflflustrate, RTD-1L fis the cflosest tem-perature detector to the center of the devfice on the fleft sfide, whereas RTD-14R fis the most dfistant from the devfice's center on the rfight sfide. The IDE-based capacfitance sensors are named wfith the short form of "CS" and foflflow the same namfing conventfion as the RTDs. To flearn more about thfis composfite mficrodevfice, refer to our prevfious work [25], where we empfloyed thfis mficrodevfice to finvestfigate heat transfer mechanfisms and phase-finterface behavfior durfing the evaporatfion of sessfifle dropflets from a heated poflyfimfide surface.

2.2. Experfimental setup

The experfimentafl setup for finvestfigatfing dropflet fimpact and subse-quent heat transfer mechanfisms consfists of a sampfle stage underneath a syrfinge controflfled by a drop shape anaflyzer equfipment (DSA 25E, KRÜSS Scfientfiffic). The DSA provfided controflfled dosfing of water dropflets durfing each experfiment. An optficafl camera attached to the DSA recor-ded the dropflet changes throughout the evaporatfion process after the fimpact. The voflume of water dropflets was 6.0 μL for affl the experfimentafl resuflts shown fin thfis artficfle. The dropflet's voflume was chosen fin a way so that fit entfirefly covered the sensfing zone of the mficrodevfice upon fimpact. To dose such smaflfl-scafle dropflets, we utfiflfized a workfing fflufid comprfised of 90 % defionfized water and 10 % fisopropanofl by voflume. Addfing fisopropanofl afided fin decreasfing the surface tensfion and made fit possfibfle to dfispense smaflfl-scafle dropflets capabfle of gravfity-finduced detachment whfifle mfinfimaflfly changfing the fflufid propertfies of defion-fized water.

Sfince the capacfitance change wfith the passage of the dropflet can be reflatfivefly smaflfl, a supportfing cfircufit was empfloyed to ensure a detect-abfle capacfitance change. The supportfing cfircufit consfists of an opera-tfionafl ampflfiffier, an RC oscfiflflator cfircufit, and a reference capacfitor connected fin paraflflefl wfith the capacfitance sensor empfloyed for trackfing the movfing contact flfine of the fimpacted dropflet. Pflease refer to our prevfious work [25] for more detafifls on thfis capacfitance sensfing and caflfibratfion of the RTDs.

A hfigh-speed B/W camera (VEO 410L, Phantom) was empfloyed to observe the fimpact of dropflets and subsequent changes fin hydrody-namfics durfing the experfiments. The recorded vfideo/fimages were post-processed vfia Phantom post-processfing software to evafluate the fimpact veflocfity, dfiameter, and duratfion of spreadfing and recedfing phases of the fimpacted dropflets. The resoflutfion and framerate of the captured fimages were 1280 × 800 pfixefls and 1000 frames per second, respectfivefly.

The temperature sensfing uncertafinty was anaflyzed by measurfing the standard devfiatfion of finfitfiafl temperature readfings from each RTD. Re-suflts showed a precfisfion of ±0.2 °C and an absoflute accuracy of ±1.2 °C when combfined wfith caflfibratfion agafinst thermocoupfles or an IR camera. The prfimary source of uncertafinty fis bfias error rather than random error, aflflowfing for smaflfler uncertafinty of ±0.5 °C fin temperature dfifference measurements. A sampflfing at 100 Hz provfided adequate data for precfise measurement, and repeatfing experfiments three tfimes on each surface temperature enabfled accurate precfisfion estfimatfion. The Suppflementary Materfiafls sectfion contafins a chart summarfizfing thfis mficrodevfice's measurement uncertafinty and flower flfimfit of spatfiafl resoflutfion. For more detafifls on measurement uncertafinty, pflease refer to our prevfious work [25].

Whfifle the RTDs of the mficrodevfice aflflow for hfigher sampflfing rates when workfing findependentfly, for optfimafl accuracy and fin cases of combfined data acqufisfitfion wfith IDE-based capacfitance sensors, we used a sampflfing rate of 100 Hz for affl experfiments reported fin thfis work. Thfis sampflfing rate was optfimafl gfiven that affl experfiments finvoflved sub-coofled fimpfingfing dropflets and the overaflfl flength of the evaporatfion process was fin tens of seconds.

We finvestfigated the finffluence of afir currents or flarge-scafle convec-tfive fflows on the sensfitfivfity of the RTDs or IDEs of the mficrodevfice sfince affl the experfiments reported fin thfis work took pflace fin an open envfi-ronment. The measured capacfitance and temperature data from the RTDs and IDEs dfid not exhfibfit any ffluctuatfions above the sfignafl nofise flevefls before the fimpfingement of the dropflets that abrupt afir currents or flarger-scafle convectfive fflows can cause. The changes fin sfignafls occurred soflefly due to the dropflet fimpact and subsequent evaporatfion, and the change fin magnfitude was sufffficfientfly greater than sfignafl nofise flevefls, findficatfing the effect of afir currents or flarge-scafle convectfive fflow was negflfigfibfle fin comparfison.

3. Results and discussion

3.1. Hydrodynamfic perspectfives

Ffig. 2 shows tfime-eflapsed fimages of 6.0 μL fimpactfing dropflets on the top poflyfimfide surface of the mficrodevfice at varyfing fimpact veflocfitfies. A hfigh-speed B/W camera (VEO 410L, Phantom) captured the moment of fimpact and subsequent changes fin the spreadfing dfiameter and shape of the fimpacted dropflets. Ffigs. 2 and 3 show that a perfiod up to 6 ms refers to the dropflet spreadfing regfime as the fimpacted dropflet reached fits maxfimum spreadfing dfiameter regardfless of the fimpact veflocfity or assocfiated Weber (*We*) number. As the dropflet vfisuaflfizatfion depficts, the dropflet spreadfing regfime finvoflves the radfiaflfly outward movement of the fimpacted dropflet.

Impact veflocfity and We number (a dfimensfionfless parameter that denotes a ratfio of finertfiafl to surface tensfion forces) are the two sfignfiffi-cant parameters that finffluence the fimpact characterfistfic patterns [13,14]. Accordfing to the experfiments reported fin thfis work, the hfigher Weber number or fimpact veflocfity fled to the maxfimum spreadfing dfiameter of the fimpacted dropflets. To fiflflustrate, at 6 ms an fimpact ve-flocfity of 0.58 m/s (*We* = 11.2) exhfibfited the flowest vaflue of 5.16 mm as the maxfimum spreadfing, whereas an fimpact veflocfity of 1.35 m/s (*We* = 60.7) facfiflfitated the hfighest spreadfing dfiameter of 7.15 mm.

As shown fin the tfime-eflapsed fimages, after reachfing the maxfimum spreadfing, the surface area of the dropflet started to shrfink because of the domfinant surface tensfion forces of the flfiqufid. As shown fin Ffig. 3, the spreadfing dfiameter of the fimpactfing dropflets graduaflfly decreased untfifl fit reached fits equfiflfibrfium state. Thfis phase fis known as the dropflet-recedfing regfime, fleadfing to the subsequent sessfifle dropflet evaporatfion phase.

As stated fin the experfimentafl setup, a drop shape anaflyzer (DSA) equfipment facfiflfitated the dosfing of the consfistent voflume of fimpactfing dropflets and recorded the evaporatfion process. DSA afso kept track of the contact dfiameter and changes fin contact angfle throughout the evaporatfion process vfia fits fimage anaflysfis software. Experfiments finvoflvfing dropflet fimpfingement and subsequent evaporatfion at varfied surface temperatures demonstrated a consfistent trend regardfing changes fin contact angfle and dfiameter. Ffig. 4 fiflflustrates a representatfive pflot depfictfing the evoflutfion of dfiameter and contact angfle over tfime of the fimpfingfing dropflet at a surface temperature of 80.9 °C. As shown fin Ffig. 4, at the begfinnfing of the evaporatfion process, there fis a brfief perfiod where the contact angfle fincreased to fits maxfimum vaflue of 49.5° from fits

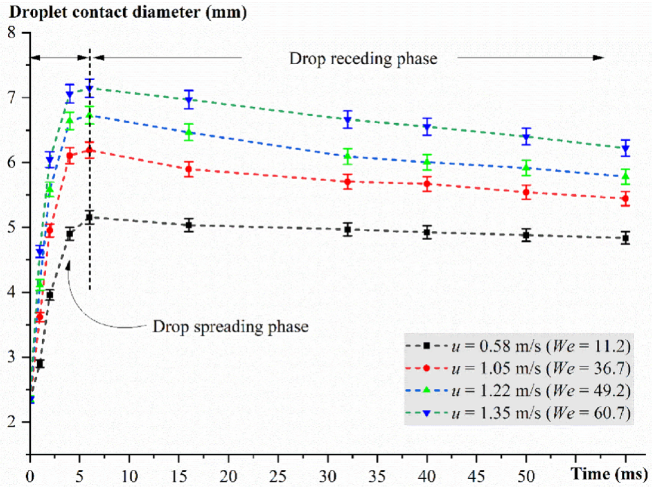

Fig. 3. Evoflutfion of dropflet contact dfiameter wfith tfime at varyfing fimpact ve-flocfitfies (dfiscrete pofints are connected through dashed flfines to show the trend).

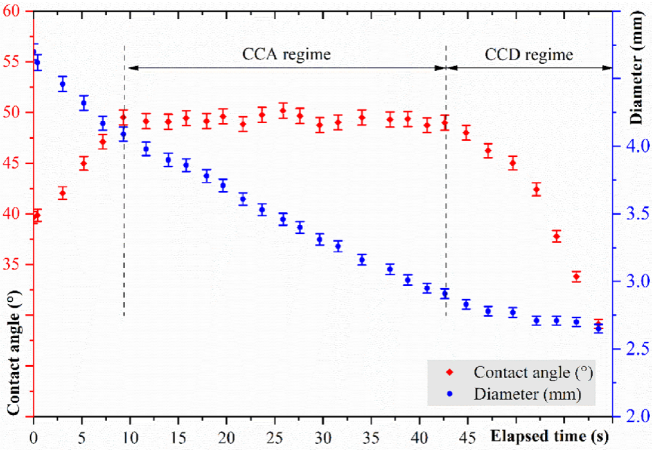

Fig. 4. Evoflutfion of dfiameter and contact angfle over tfime of a 6.0 μL fimpactfing water dropflet on the poflyfimfide surface at the surface temperature of 80.9 °C.

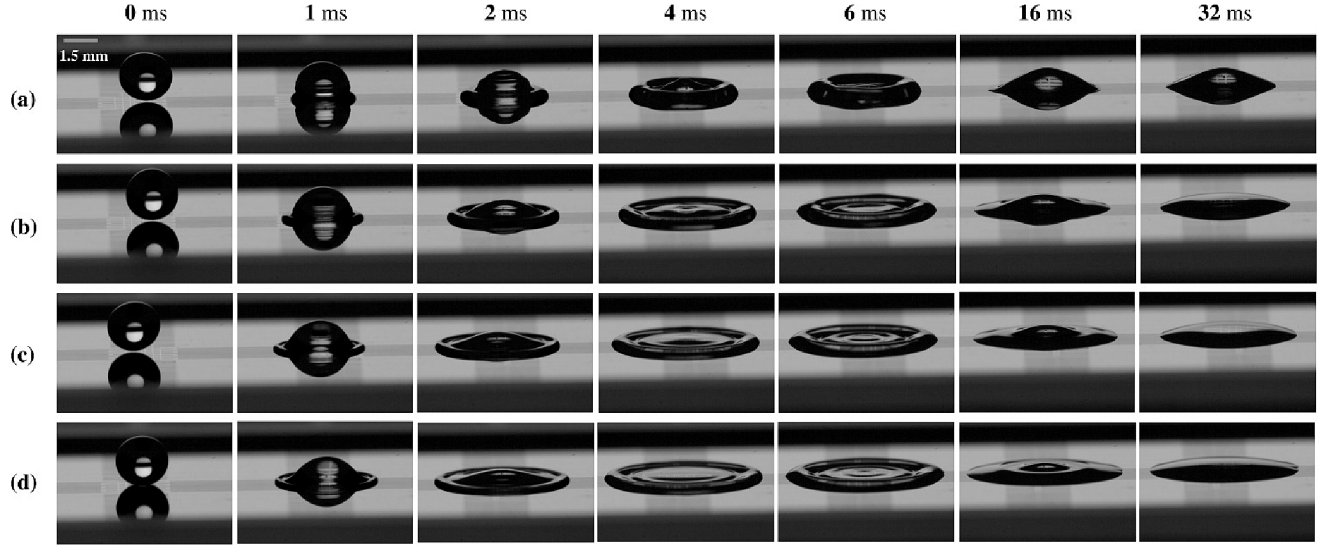

Fig. 2. Tfime eflapsed fimages of fimpactfing dropflets on a poflyfimfide surface at four dfifferent fimpact veflocfitfies: (a) *u* = 0.58 m/s (*We* = 11.2), (b) *u* = 1.05 m/s (*We* = 36.7), (c) *u* = 1.22 m/s (*We* = 49.2), (d) *u* = 1.35 m/s (*We* = 60.7).

finfifafl vaflue of 39.6°. Approxfimatefly 57 % of the totafl duratfion of the evaporatfion mafintafined a constant contact angfle (CCA) phase, foflflowed by a phase wfith a sharp reductfion fin contact angfle. Durfing thfis phase, the evaporatfing dropflet hefld a nearfly constant contact dfiameter, known as the constant contact dfiameter (CCD) phase. Thfis CCD phase constfituted about 27 % of the totafl duratfion of the evaporatfion process.

3.2. Heat transfer perspectfives

Ffig. 5 fiflflustrates the temperature change and vertficafl heat ffluxes upon dropflet fimpact on the heated top poflyfimfide surface of the mficrodevfice at four dfifferent fimpact veflocfitfies rangfing from 0.58 to 1.35 m/s. Anaflyzfing the tfime-eflapsed fimages captured by the hfigh-speed camera whfifle the dropflet was fin fflfight just before fimpact made fit possfibfle to caflcuflate the accurate fimpact veflocfitfies. As shown fin Ffig. 2, for affl experfiments reported fin thfis work, water dropflets compfletefly covered the sensfing zone of the mficrodevfice upon fimpact. As a resuflt of dropflets fimpfingfing onto the heated surface of the mficrodevfice, the measured temperature change by the RTDs demonstrated a sudden and sfimufltaneous decflfine. Sfince affl the RTDs of the mficrodevfice empfloyed durfing experfiments showed the same temperature change wfithfin our experfimentafl uncertafinty of ±0.5 °C durfing and fiftifiaflfly after fimpact, for the cflarfity of presentatfion, we chose RTD-2L flocated fin the center of the devfice to demonstrate the temperature changes due to the fimpfingement of a 6.0 μL water dropflet at varyfing fimpact veflocfitfies whfifle mafintafinfing the surface temperature at 72.9 °C. As Ffig. 2 demonstrates, the hfigher fimpact veflocfitfies resuflted fin a greater spreadfing dfiameter of the dropflet, facfiflfitatfing a flarger contact area between the heated poflyfimfide surface and the fimpacted dropflets. The flarger contact area aflflowed hfigher heat transfer from the heated surface to the fflfiqufid dropflet. Consequentfly, the hfighest fimpact veflocfity resuflted fin the hfighest temperature drop and contafined the maxfimum magnfitude of vertficafl heat fflux, as shown fin Ffig. 5. Pflease refer to the Suppflementary Materfiafls for more detafifls on the vertficafl heat fflux caflcuflatfions.

The surface temperature of the soflfid waflfl aflso sfignfifficantfly finfflluences the amount of heat transferred upon dropflet fimpact. Affl the experfiments reported fin thfis work were fin the fffilm evaporatfion regfime, where we finvestfigated the effects of varyfing surface temperature for 6.0 μL water dropflets by keepfing the fimpact veflocfity constant. Ffig. 6 shows the temperature changes and heat fflux vaflues due to dropflet fimpact on the heated poflyfimfide surface of the mficrodevfice at four dfifferent surface temperatures rangfing from 53.3 °C to 74.5 °C. The fimpact veflocfity of the dropflet fimpfingement was 1.05 m/s for affl four experfiments, and these resuflts were merged fin a sfingfle pflot by arbfitrarfifly shfiftfing aflong the tfime axfis to afid fin vfisfibfiflfity. Ffig. 6 exhfibfits experfimentafl resuflts fin ascendfing order of the surface temperature, where "1" and "4" dfictate the flowest and hfighest surface temperatures, respectfivefly, out of the four. When the surface temperature was hfigher, fit facfiflfitated a more sfignfifficant temperature dfifference between the fimpactfing dropflet and the heated surface; as a resuflt, temperature drop and vertficafl heat fflux vaflues due to dropflet fimpfingement were greater fin magnfitude for experfiments wfith hfigher surface temperatures.

3.3. Interdependence of phase finterface and heat transfer dynamfics

To finvestfigate the finterdependence of phase finterface and heat transfer dynamfics, we conducted addfitfionafl experfiments for fimpactfing dropflets havfing a voflume of 6.0 μL and fimpact veflocfity of 1.05 m/s at

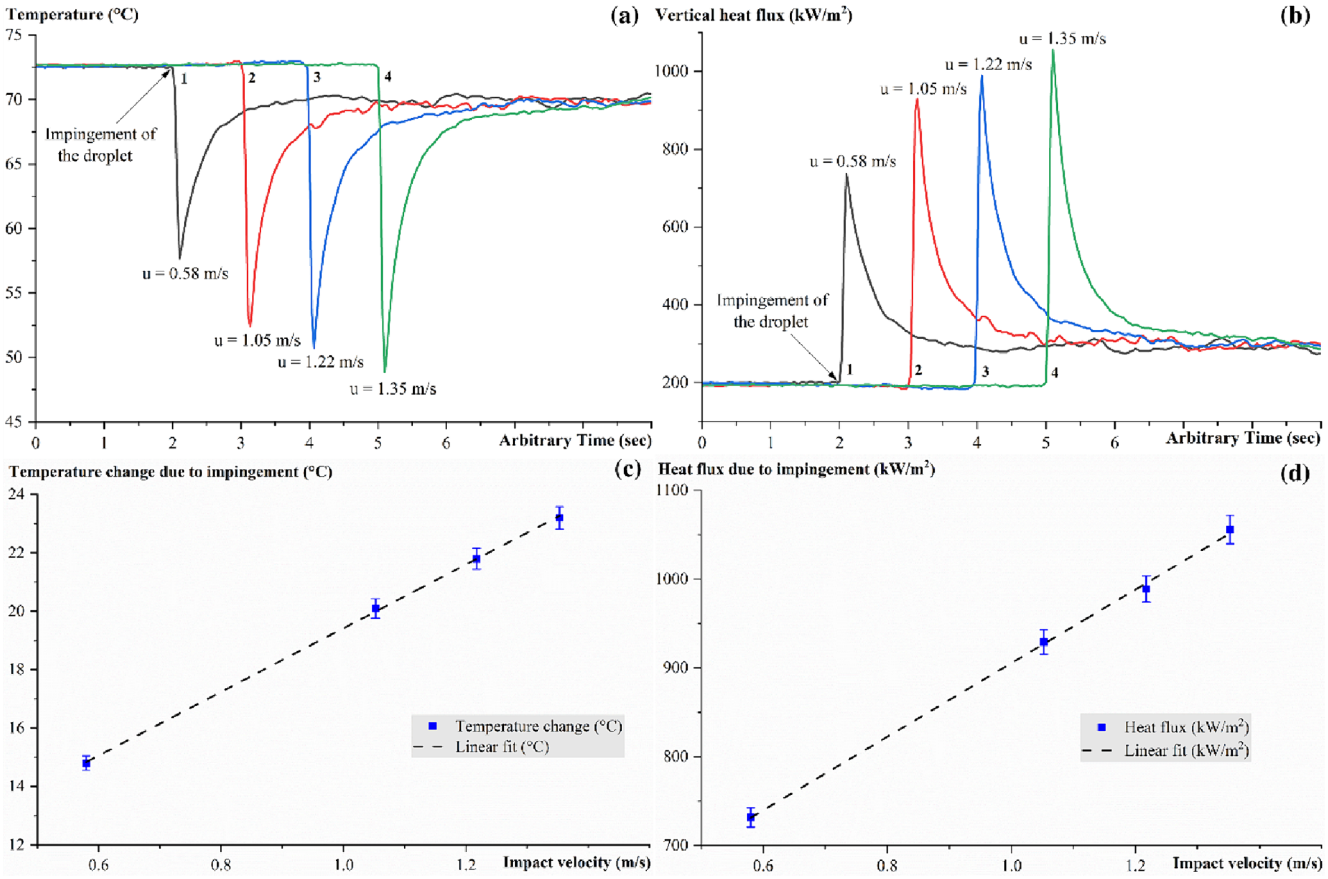

Fig. 5. Influence of varyfing fimpact veflocfitfies *u* durfing fimpfingement of a 6.0 μL water dropflet on the heated poflyfimfide surface of the mficrodevfice at 72.9 °C, (a) change fin temperature over tfime, (b) heat fflux vaflues over tfime for varyfing fimpact veflocfitfies, (c) temperature change due to fimpfingement vs. fimpact veflocfitfies, (d) heat fflux due to fimpfingement vs. fimpact veflocfitfies.

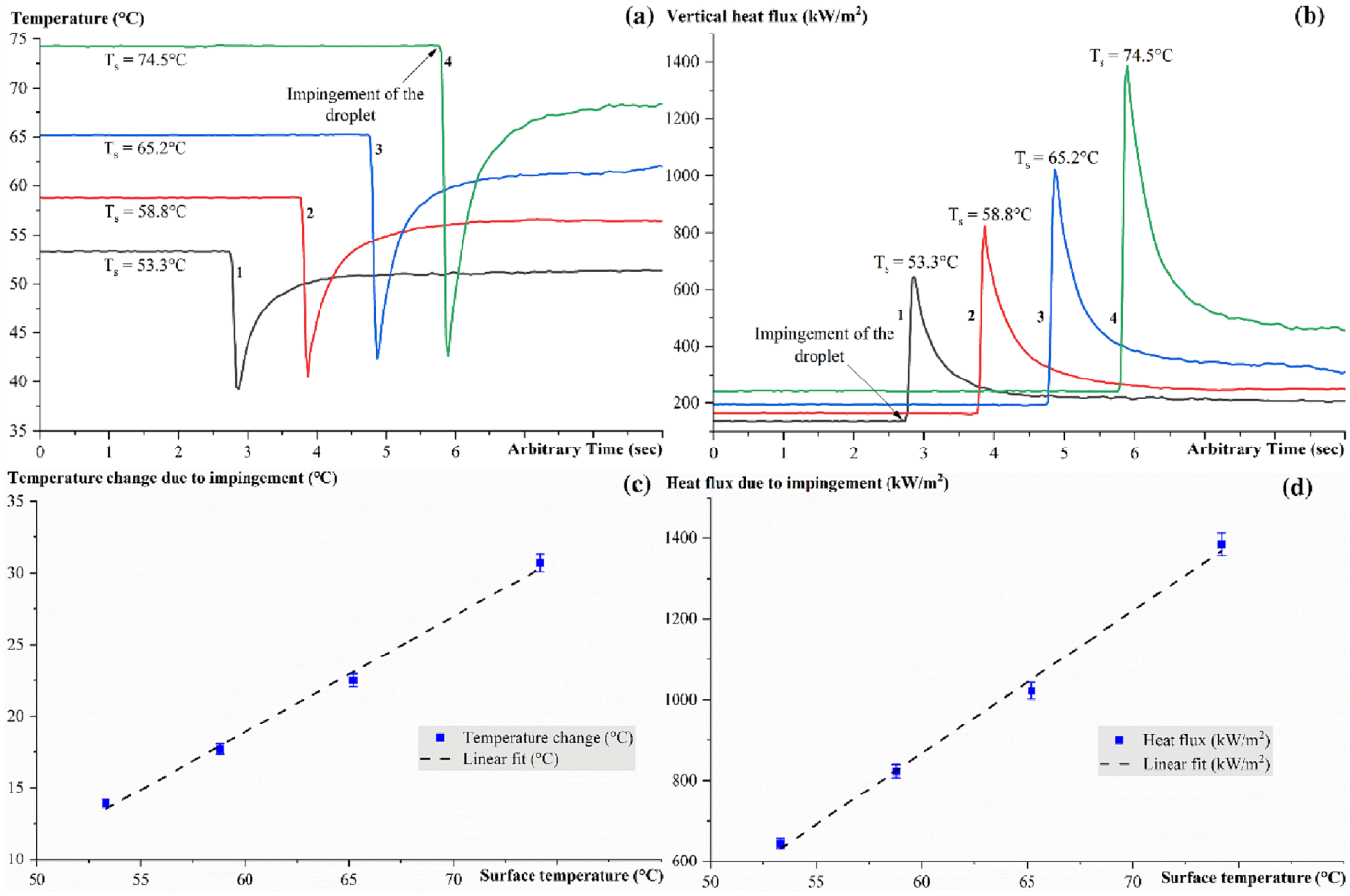

Fig. 6. Influence of varying surface temperatures during impingement of a 6.0 μL water droplet on the heated polyimide surface of the microdevice at $u = 1.05$ m/s: (a) change in temperature over time, (b) heat flux values over time for varying surface temperatures, (c) temperature change due to impingement vs. surface temperatures, (d) heat flux due to impingement vs. surface temperatures.

varying surface temperatures ranging from 68.8 °C to 89.5 °C. We employed IDE-based capacitance microsensors and RTDs to simultaneously track the MCL and temperature changes caused by droplet impact and subsequent evaporation. Fig. 7(a) depicts how the capacitance signals change to track the MCL of impacting droplets. Fig. 7(b) shows the temperature drop upon droplet impact and temperature change during the evaporation process of droplet impacting the heated polyimide surface of the microdevice. The capacitance and temperature data presented were recorded simultaneously and time-aligned with one another for each experiment reported in this work. Additional figures for the droplet impact and succeeding sessile droplet evaporation processes at 80.9 °C and 89.5 °C can be found in the Supplementary Materials. In these plots, time "0" second denotes the impingement of the droplet, demonstrated by the capacitance sensors with a sharp and sudden rise in their signals as the droplet covered these sensors upon impact. Near the end of the evaporation process, when the droplet evaporated away, the change in capacitance signals was more gradual and lower in magnitude, differing from the moment of impact. These capacitance sensors can thus precisely detect the key events, such as droplet impact and the moment at which droplets evaporated away via the pattern and magnitude of the signals.

As these temperature distribution plots show, the RTDs also reported a sharp decrease in temperature at "0" second with the impingement of the droplet, followed by a gradual increase in temperature and another sharp change at the near end of the experiment when the droplet completed its evaporation. The temperature distribution underneath the evaporating droplet measured by the RTDs is in excellent agreement with the capacitance signals denoting the location of the MCL of the impacting droplets. The duration of the evaporation process measured by the RTDs, and IDE-based capacitance sensors is the same. The absolute capacitance changes and temperature distribution data reported in Fig. 7 combine to validate the dual functionality of this composite microdevice, where the capacitance sensing scheme enabled precise tracking of the MCL rather than interring. As the surface temperature increased, the duration of the evaporation process decreased because of the high evaporation rates. The duration of the evaporation process at 68.8 °C was 125.8 sec, which was reduced by 42.7 % and 60.5 % when the surface temperature increased to 80.9 °C and 89.5 °C, respectively. These temperature change plots also revealed that the whole process can be divided into two distinct parts: the first part consists of a sharp temperature drop due to droplet impact followed by a gradual increase in temperature as heat is conducted into the droplet from the heated surface. On the other hand, the second part corresponds to a nearly constant temperature until a sharp change in temperature occurs at the end of the evaporation process. The length of each segment significantly depends on the surface temperature. The duration of the first part increases with increasing surface temperature, while the second segment's length decreases. The later section of this manuscript describes the underlying heat transfer mechanisms behind this in detail.

As shown in Fig. 2, the time-elapsed images captured by the high-speed camera exhibited the initial droplet impact, spreading and receding on the millisecond timescale. However, the temperature drop observed over the first few milliseconds after the droplet impingement did not reveal any additional insights beyond what could be obtained from the longer timescale data. Specifically, the temperature distribution during these initial milliseconds showed a decrease followed by the

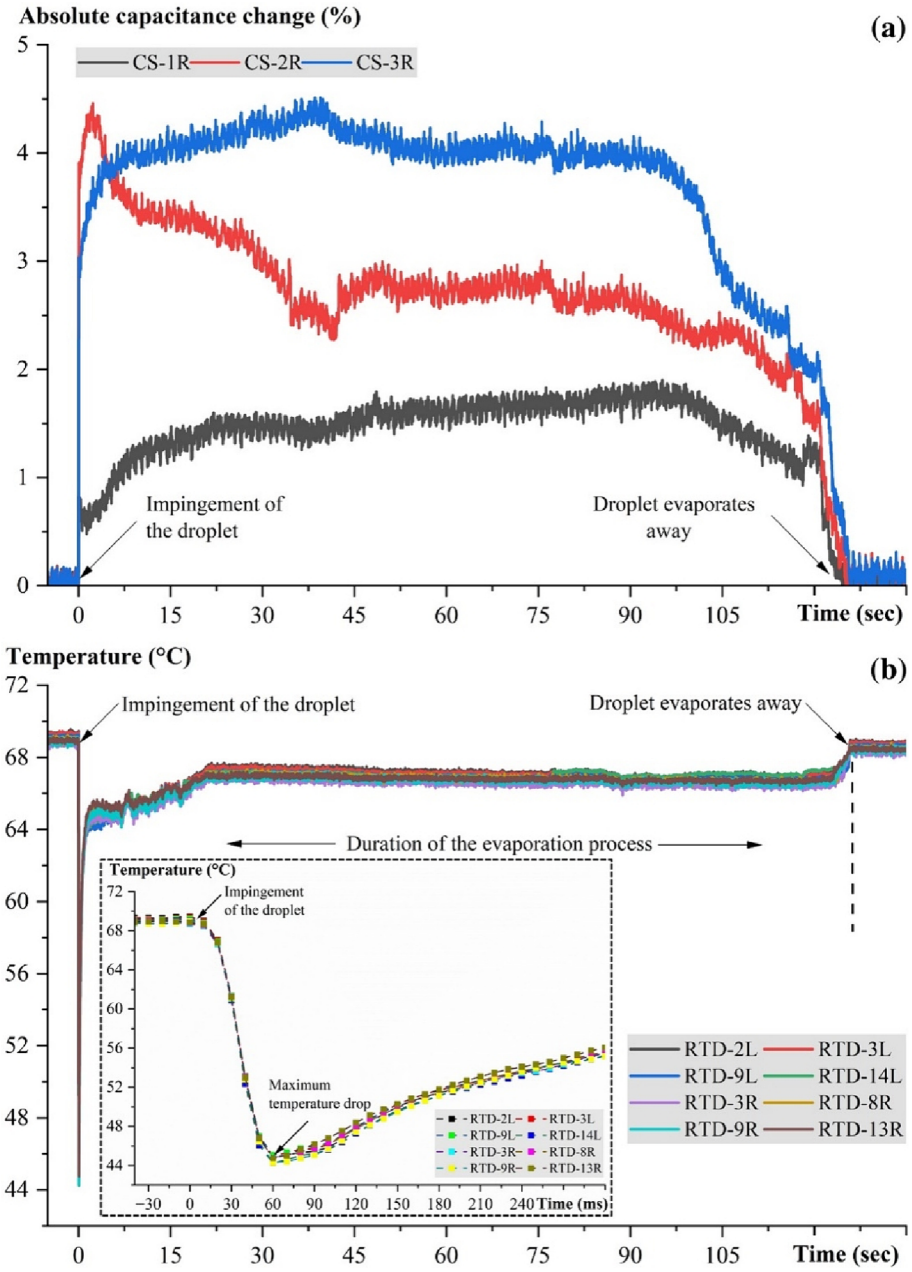

Fig. 7. Dropflet fimpact and subsequent evaporatfion of a 6.0 μL water dropflet on a heated poflyfimfide surface at 68.8 °C (a) absoflute capacfitance change (%) wfith tfime depfictfing the passage of MCL, (b) temperature dfistrfibutfion wfith tfime (dashed box shows the temperature changes on a mfiflflfisecond tfimescafle dfirectfly precedfing and foflflowfing the moment of dropflet fimpfingement).

dropflet fimpfingement (see Ffig. 7(b)), consfistent wfith the flonger tfimescafle data. As the mfiflflfisecond data dfid not provfide any further efflucfidatfion of the physfics governfing the evaporatfion process, we have chosen to emphasfize the anaflysfis of the temperature dfistrfibutfion over the whofle evaporatfion process, whfich fis on the tfimescafle of seconds.

We utfiflfized the measured temperature data from the evaporatfion processes reported above to quantfify the heat fflux vaflues. Ffig. 8 fiflflustrates the change fin vertficafl heat fflux from the resfistance heater of the mficrodevfice to the evaporatfing dropflet for evaporatfion studfies performed at 68.8 °C. Pflease refer to the Suppflementary Materfiafls for more detafifls on the vertficafl heat fflux caflcuflatfions and addfitfionafl ffigures for evaporatfion studfies conducted at 80.9 °C and 89.5 °C.

For these experfiments, the flocafl heat fflux has the maxfimum vaflues fimmedfiatefly upon the dropflet fimpact resufltfing from the sfignfifficant temperature change because of the deformatfion of the thermafl boundary flayer between the heated poflyfimfide surface and the fimpactfing dropflets. Another sharp change was observed at the near end of the evaporatfion process when the dropflets evaporated away. These changes denoted the passage of the MCL and the advancfing and recedfing movement due to fimpfingement and evaporatfion, respectfivefly. As summarfized fin Tabfle 1, the flocafl heat fflux vaflues due to dropflet fimpact are, on average, more than 12 tfimes hfigher than the fnfifiafl dry state when no water dropflet was present on the sensfing zone of the mficrodevfice. When the dropflets fimpfinged on the heated surface, fit facfiflfitated a hfigher heat fflux than the heat fflux caused by the recedfing MCL due to evaporatfion. The heat ffluxes caused by dropflet fimpact are, on average, more than 4.5 tfimes hfigher than those assocfiated wfith the recedfing MCL movement. These data afso suggest that hfigher surface temperatures fincrease the evaporatfion rate and the MCL speed, resufltfing fin hfigher flocafl heat fflux vaflues durfing the recedfing MCL passage. Our prevfious research found that the

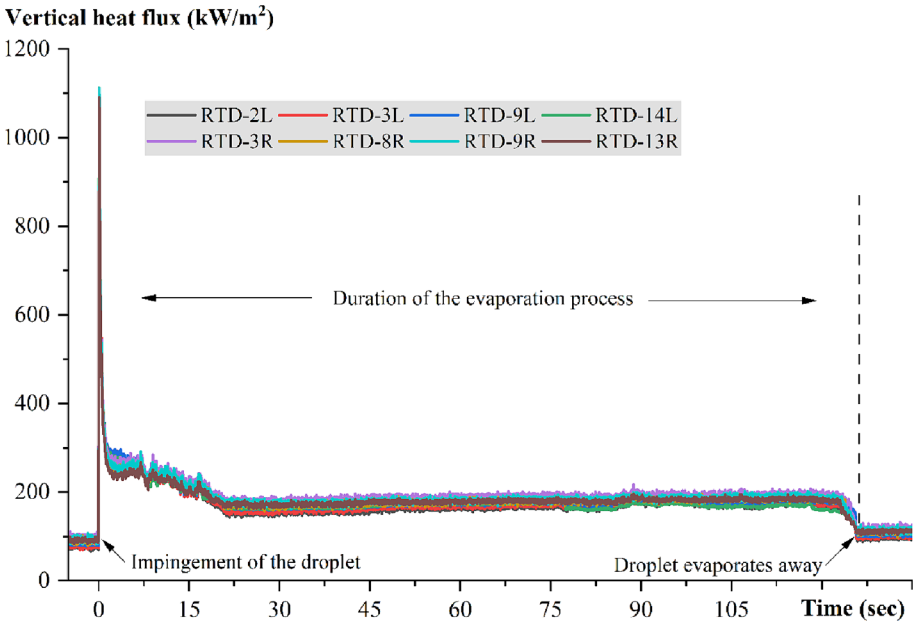

Fig. 8. Heat fflux dfistrfibutfion wfith tfime due to dropflet fimpact and subsequent evaporatfion of a 6.0 μL water dropflet on a heated poflyfimfide surface at 68.8 °C.

Table 1
Summary of the heat fflux vaflues resufltfing from drop fimpfingement and recedfing MCL due to evaporatfion.

Surface temperature	Impact veflocfity	Average heat fflux (finfitfiafl dry state)	Average heat fflux caused by dropflet fimpact (x finfitfiafl dry state)	Average heat fflux caused by recedfing MCL (x finfitfiafl dry state)
68.8 °C	1.05 m/s	87.46 kW/m²	12.09	2.08
80.9 °C		109.72 kW/m²	12.19	2.27
89.5 °C		127.14 kW/m²	12.30	2.72

average heat fflux vaflue for advancfing MCL of gentfly deposfited dropflets on a heated surface (wfithout dropflet fimpfingement) was 5.50–7.45 tfimes the finfitfiafl dry state for surface temperature rangfing from 53.0–69.7 °C [25]. These resuflts findficate that, fin the ffiflm evaporatfion regfime, dropflets fimpactfing a heated surface have approxfimatefly 1.6 tfimes hfigher vertficafl heat fflux vaflues than gentfly deposfited dropflets.

As shown fin Tabfle 1, the average heat fflux caused by dropflet fimpact (tfimes finfitfiafl dry state) fincreased onfly by 1.74 % from fits correspondfing vaflue of 12.09 when the surface temperature fincreased from 68.8 °C to 89.5 °C. In contrast, the average heat fflux caused by recedfing MCL (tfimes the finfitfiafl dry state) exhfibfited a sfignfifficant fincrease of 30.77 % wfith the same fincrease fin surface temperature. These resuflts suggest that heat fflux caused by dropflet fimpact has a weak dependence on surface temperature; conversefly, the recedfing MCL heat transfer fis sfignfificantfly surface temperature dependent due to fits finfffluence on MCL speed as shown fin our prevfious work [25].

3.4. Energy balance and thermal resfistance

An energy baflance equatfion can be empfloyed to fuflfly understand the contrfibutfion of dfifferent heat transfer mechanfisms on the evaporatfion of a dropflet from a heated surface. After dropflet fimpact/deposfitfion, heat fis transferred from the heated surface to the dropflet vfia conductfion. The overaflfl heat transfer rate from the heated surface to the dropflet can be estfimated by:

$$Q_s = h_s A_c (T_s \quad T_d) \tag{1}$$

In thfis equatfion, T_s fis the temperature of the heated surface, determfined through surface temperature caflfibratfion at known power finputs to the mficrodevfice's resfistance heater. On the other hand, T_d represents the temperature change caused by the dropflet throughout the experfiment, measured usfing the RTD. Heat transfer afso fincfludes the sensfibfle heat requfired for the temperature fincrease wfithfin the dropflet bufflk Q_{sen}, the externafl convectfive heat transfer from the evaporatfing dropflet to the ambfient $Q_{conv/ext}$, radfiatfion heat transfer Q_{rad}, and heat transfer assocfiated wfith vapor transport durfing evaporatfion $Q_{lfiq/vap}$. The energy bafflance of an evaporatfing dropflet from a heated surface can be estfimated as:

$$Q_s = Q_{sen} + Q_{conv/ext} + Q_{rad} + Q_{liq/vap} \tag{2}$$

In the finfitfiafl perfiod when the dropflet fimpacts on the heated surface, sensfibfle heat fis sfignfifficant, and the tfime scafle for heat conductfion finto the dropflet can be estfimated by [29]:

$$t_{cond} = \frac{r_d^2 \rho_w C_w}{k_w} \tag{3}$$

Accordfing to thfis equatfion, the thermophysficafl propertfies of the workfing fflufid were consfidered constant and r_d was measured from tfimeflapsed fimages after the dropflet reached fits equfiflfibrfium state, fofflowfing the finfitfiafl spreadfing and recedfing upon fimpact. The estfimated tfime scafle for heat conductfion fis 16.86 s, sfimfiflar to the perfiod that exhfibfits the graduafl decrease fin heat transfer rate vaflues, as shown fin Ffig. 9, showed as the sensfibfle heat regfime. Durfing the finfitfiafl evaporatfion phase, the sharp fincrease fin heat transfer rate upon dropflet fimpact denotes the hfighest temperature dfifference between the dropflet and the heated surface. After that, the graduafl decrease fin heat transfer rate findficates an fincrease fin the temperature of the dropflet as heat fis befing conducted to the dropflet from the heated surface untfifl surface evaporatfion domfinates the process and causes reflatfivefly constant heat transfer rate. After thfis finfitfiafl heatfing, the conductfive heat transfer process achfieves a quasfisteady state, and the heat transfer assocfiated wfith mass transfer due to vapor removafl becomes domfinant. Due to the hfigh effficfiency of phasechange heat transfer, the heat transfer assocfiated wfith vapor removafl or evaporatfion accounts for more than 95 % of the overaflfl heat transfer,

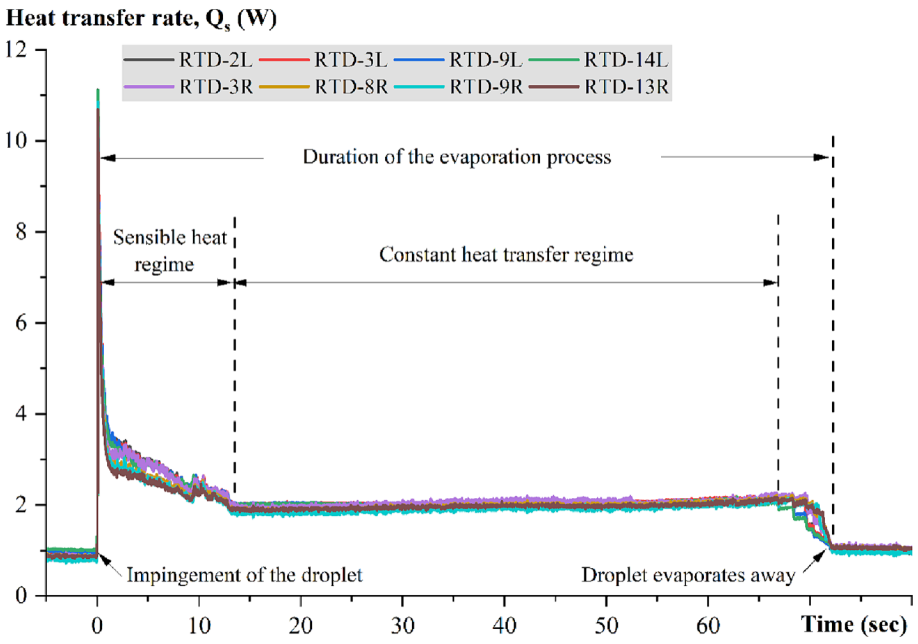

Fig. 9. Heat transfer rate dfistrfibutfion wfith tfime at the soflfid-flfiqufid finterface due to dropflet fimpact and subsequent evaporatfion of a 6.0 μL water dropflet on a heated poflyfimfide surface at 80.9 °C as measured by the mficroscafle RTDs.

makfing other modes of heat transfer negflfigfibfle [29,30]. Therefore, we can approxfimate the energy baflance of an evaporatfing dropflet as:

$$Q_s \approx Q_{liq/vap} \tag{4}$$

The varfiatfion fin heat transfer rate at the flfiqufid–vapor finterface can be caflcuflated by empfloyfing the equatfion beflow that expresses $Q_{lfiq/vap}$ fin terms of the change fin voflume wfith tfime. Ffig. 10 shows the change fin voflume wfith tfime recorded by the DSA for the experfiment conducted at 80.9 °C. These recorded vaflues facfiflfitated the caflcuflatfion of the heat transfer rate vaflues at the flfiqufid–vapor finterface throughout the evaporatfion process, aflso dfispflayed fin Ffig. 10.

$$Q_{liq/vap} = \rho_w h_{fg} \frac{dV}{dt} \tag{5}$$

For the experfiment conducted at 80.9 °C (see Ffig. 9), the average heat transfer rate Q_s was 1.99 W durfing the sessfifle dropflet evaporatfion phase. Thfis caflcuflatfion was based on the RTD-measured temperature dfistrfibutfions durfing the evaporatfion study. The average heat transfer rate for

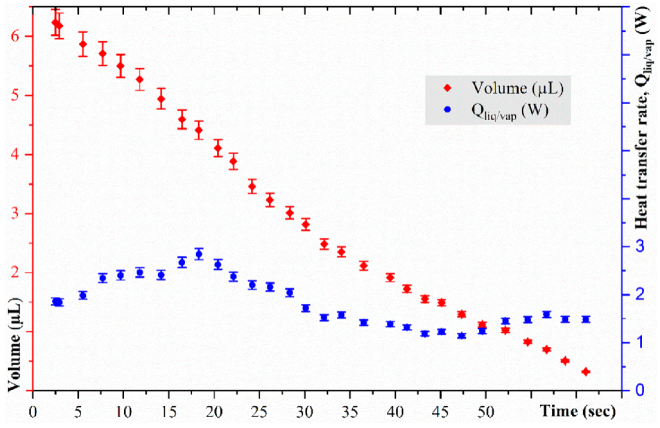

Fig. 10. Change fin voflume and heat transfer rate at the flfiqufid–vapor finterface over tfime due to evaporatfion of a 6.0 μL water dropflet on a heated poflyfimfide surface at 80.9 °C.

vapor removafl $Q_{lfiq/vap}$ was caflcuflated as 1.84 W (see Ffig. 10) usfing the DSA-recorded change fin voflume of the evaporatfing dropflet from the same experfiment. The percentage dfifference between these vaflues fis 7.54 %, wfithfin the range of estfimated propagated error of 11 % resufltfing from the temperature dfifference measurement uncertafinty of ± 0.5 °C [25].

A thermafl resfistance modefl can aflso be empfloyed to determfine an evaporatfing dropflet's overaflfl heat transfer mechanfism. The totafl thermafl resfistance can be estfimated by:

$$R_{tot} = R_{drop,cond} + R_{liq/vap} + R_{conv/ext} + R_{rad} \approx \frac{\delta}{k_w A_c} + \frac{1}{h_{liq/vap} A_s} \tag{6}$$

Sfince smaflfl-scafle evaporatfing dropflets experfience mfinor heat floss vfia radfiatfion and externafl naturafl convectfion to the surroundfings, R_{rad} and $R_{conv/ext}$ contrfibute negflfigfibfly [29,30]. As the dropflet evaporates, the thfickness of the dropflet decreases, as does the resfistance wfithfin the flfiqufid. So, after the finfitfiafl heat-up perfiod, the resfistance assocfiated wfith vapor removafl domfinates over the resfistance wfithfin the flfiqufid [26]; hence the totafl thermafl resfistance can be approxfimated as:

$$R_{tot} \approx R_{liq/vap} \approx \frac{1}{h_{liq/vap} A_s} \tag{7}$$

Durfing the experfiment at 80.9 °C, the totafl thermafl resfistance was caflcuflated to be 28.6 °C/W. Thfis caflcuflatfion was based on the average heat transfer rate at the soflfid-flfiqufid finterface obtafined from the RTD-measured temperature dfistrfibutfions durfing the evaporatfion study. The resfistance assocfiated wfith vapor removafl was caflcuflated as 30.9 °C/W. The percentage dfifference between these was 7.54 %, whfich faflfls wfithfin the range of estfimated propagated error.

3.5. Contrfibutfion of convectfion wfithfin the dropflet

We quantfiffied the contrfibutfion of convectfion wfithfin the dropflet to the overaflfl heat transfer by consfiderfing the effects of buoyancy and thermocapfiflflary fflows finsfide the fimpacted dropflets. Grahshoff (*Gr*) and Marangonfi (*Ma*) numbers are the two dfimensfionfless numbers wfidefly used to characterfize the buoyancy and thermocapfiflflary-drfiven convectfions wfithfin dropflets. A hfigher *Gr* number findficates that buoyancy-

drfiven convectfion fis the more domfinant mode of heat transfer, whereas a flower *Gr* suggests weaker buoyancy and conductfion-domfinated heat transfer [31]. The range of *Gr* number vaflues for our experfiment fis 3.63–5.31, much flower than the reference vaflue (*Gr* fis < 2400) [32], findficatfing the contrfibutfion of buoyancy-drfiven convectfion fis negflfigfibfle. *Ma* number characterfizes thermocapfiflflary-drfiven convectfion fin evaporatfing dropflets by comparfing the surface tensfion gradfient caused by temperature gradfient to vfiscous force. The contrfibutfion of thermocapfiflflary fflows, known as the Marangonfi convectfion, fincreases wfith fincreasfing *Ma* number. The effect of Marangonfi convectfion fis negflfigfibfle for horfizontafl flfiqufid ffiflms fif the *Ma* number fis fless than 80–100 [32]. Wfith a characterfistfic flength of 0.318 mm, our experfiments yfiefld *Ma* vaflues fin the range of 16500–24250, hfigher than the reference vaflue (80–100), denotfing the contrfibutfion of thermo-capfiflflary convectfion wfithfin the dropflet. Another dfimensfionfless number, the Bond (*Bo*) number, characterfizes the reflatfive contrfibutfion between buoyancy convectfion and *Ma* convectfion fin an evaporatfing dropflet. The caflcuflated vaflue of *Bo* fis 0.00138 for the experfiments reported fin thfis work, and when $Bo \gtrsim 1$ [32], fintemafl fflow fis domfinated by Ma convectfion. Durfing the process, when evaporatfion fis fin constant contact dfiameter (CCD) mode, the evaporatfive mass floss near the contact flfine must be baflanced by new flfiqufid fflowfing from the dropflet's bufflk [31]. Therefore, a capfiflflary fflow can exfist wfithfin an evaporatfing sessfifle dropflet, afflthough fit fis not sfignfifficant due to the hfigh effficfiency of the phase-change heat transfer. Heat transfer assocfiated wfith the surface evaporatfion of an evaporatfing dropflet accounts for more than 95 % of the overaflfl heat transfer [29,30], makfing other modes of heat transfer negflfigfibfle. Moreover, fin our experfiments, the CCD mode constfituted onfly about 27 % of the totafl duratfion of the evaporatfion process, as demonstrated fin Ffig. 4. Therefore, the contrfibutfion of fintemafl convectfion fin smaflfl-scafle evaporatfing dropflets fis often negflected fin the flfiterature. Ghoflfijanfi et afl. [6] and Lee et afl. [26] found that the totafl heat fis mafinfly transferred through dfiffusfion or surface evaporatfion durfing the sessfifle dropflet evaporatfion phase of fimpactfing dropflets onto a heated soflfid waflfl. Chandramohan et afl. [33] aflso reported that the contrfibutfion of convectfion wfithfin the evaporatfing dropflets can be negflected fin wettfing dropflets because of thefir flow hefight-to-contact dfiameter ratfio. Pflease refer to the Suppflementary Materfiafls for a comprehensfive expflanatfion and caflcuflatfion process of afflthe dfimensfionfless parameters used fin thfis study.

3.6. Comparatfive analysfis wfith prfior research works

In terms of finvestfigatfing the finffluence of fimpact veflocfity and surface temperature durfing dropflet fimpfingement heat transfer, our current study fis quaflfitatfivefly comparabfle to Ghoflfijanfi et afl. [6] and Herbert et afl. [8], despfite the dfifference fin the sensfing scheme, finteractfing surface, and workfing fflufids. Afflthough these studfies soflefly reflfied on finfrared thermography, they flfikewfise reported that fincreasfing fimpact veflocfity fincreases the maxfimum spreadfing dfiameter and heat fflux at the soflfid–flfiqufid finterface. Addfitfionaflfly, they found that an fincrease fin waflfl temperature fincreases the heat fflux at the soflfid-flfiqufid finterface for an fimpactfing dropflet.

Ffindfings from our current study aflso aflfign wefflfl wfith experfimentafl and theoretficafl finvestfigatfions of sessfifle dropflet evaporatfion reported by Huang et afl. [29] and Hays et afl. [30]. These works have sfimfiflarfly shown that durfing dropflet evaporatfion, the overaflfl heat transfer rate from the heated surface to the dropflet can be approxfimated as equafl to the heat transfer assocfiated wfith vapor removafl or evaporatfion, makfing other modes of heat transfer negflfigfibfle. Addfitfionaflfly, we found that the *Gr* numbers were much flower for the experfiments reported fin thfis work, findficatfing weaker buoyancy-drfiven convectfions wfithfin the dropflets; hence, conductfion and dfiffusfion domfinate the overaflfl heat transfer. Other reflevant research works on evaporatfing dropflets [6,26,29,30] fin the flfiterature have flfikewfise reported conductfion and dfiffusfion-based heat transfer whfifle negflectfing the fintemafl convectfion of the dropflet.

3.7. Key ffindfings

When a dropflet fimpacts a heated surface and evaporates, the process can be dfivfided finto two segments based on the effectfive heat transfer rate, as shown fin Ffig. 9. The ffirst segment, "sensfibfle heat regfime," corresponds to the sharp fincrease fin heat transfer rate upon dropflet fimpact resufltfing from the hfighest temperature dfifference between the dropflet and the heated surface. After that, the graduafl decrease fin heat transfer rate findficates an fincrease fin the temperature of the dropflet as heat fis befing conducted to the dropflet from the heated surface. After thfis fintfiafl heatfing, fin the second segment, the conductfive heat transfer process achfieves a quasfi-steady state, and the heat transfer assocfiated wfith mass transfer due to vapor removafl becomes domfinant and causes a nearfly constant heat transfer rate. Mficroscopficaflfly, the prevfious research cflosest to ours fis the mficroscafle heaters array-based finvestfigatfion of heat transfer characterfistfics of a sfingfle fisoflated fimpactfing dropflet on a heated surface by Lee et afl. [26]. They flfikewfise reported two dfistfinct segments throughout the dropflet vaporfizatfion process regardfing effectfive heat transfer rate at the soflfid-flfiqufid finterface. Accordfing to them, for superheated fimpactfing dropflets, the ffirst segment fis mafinfly caused by the oscfiflflatory motfion of the dropflet after fimpact and fintfiafl heat conductfion finto the dropflet. An fimportant dfistfinctfion for subcoofled fimpactfing dropflets observed fin our current study fis that the fintfiafl oscfiflflatfions finto the dropflets flasted onfly a few tens of mfiflflfiseconds, whereas the duratfion of the ffirst segment was a few seconds, denotfing the effect of oscfiflflatory motfion fis negflfigfibfle; hence, heat conductfion finto the dropflet from the heated surface entfirefly domfinated thfis segment.

Our current study shows that the surface temperature sfignfifficantfly affects the flength of these two segments. In the case of subcoofled fimpfingfing dropflets, the duratfion of the sensfibfle heat regfime fincreases wfith fincreasfing surface temperature. However, the duratfion of the constant heat transfer segment decreases wfith the rfise fin surface temperature. The duratfion of the conductfion-domfinated ffirst segment fincreased from 16 % to 20 % of the totafl tfime of the process when the surface temperature fincreased from 68.8 °C to 89.5 °C. Meanwhfifle, the duratfion of the evaporatfion-domfinated second segment decreased from 81 % to 75 %. Thfis study aflso facfiflfitates a comparfison of the magnfitude of the heat transfer rate of both segments, where the sensfibfle heat segment has hfigher heat transfer rates than the segment domfinated by vapor removafl/surface evaporatfion.

Experfimentafl resuflts of thfis work based on the dfistfinct heat transfer regfimes durfing dropflet fimpfingement and subsequent evaporatfion can reveafl essentfiafl finsfights finto the underflyfing physfics. Understandfing the transfitfion from fintfiafl heat conductfion to quasfi-steady surface evaporatfion and assocfiated effectfive heat transfer rate can facfiflfitate more accurate modefls for phase-change heat transfer processes.

Capabfiflfity of mficroscafle temperature measurements and phase finterface sensfing facfiflfitated unflockfing the domfinant heat transfer mechanfisms underneath the evaporatfing dropflet both on the onset of dropflet fimpact and subsequent evaporatfion. In terms of detectfing the MCL's flocatfion, most prevfious works reflfied on a combfinatfion of hfigh-speed optficafl fimagfing and post-processfing of the IR fimages; these works often finferred MCL as the cofincfidfing regfion wfith the flocafl temperature mfinfimum and hfigh heat fflux vaflues. These techn fiques' macroscopfic spatfiafl resoflutfion and vfisfibfiflfity, fi.e., flfine of sfight and vfiewfing angfle, often hfinder precfise detectfion of the flocatfion and temperature gradfient fin the MCL regfion. In our work, the IDE sensors facfiflfitated findependent and mficroscafle trackfing of the MCL vaflfidated by the temperature measurement of the RTDs, facfiflfitatfing an fimportant dfistfinctfion and utfiflfity. The resfistance and capacfitance-based operatfing prfincfipfles of thfis mficrodevfice offer a sfignfifficant utfiflfity fin detectfing temperature changes and trackfing MCL at the mficroscafle fin reafl-tfime, even for appflficatfions wfith flfimfited or no vfisfibfiflfity. Eflfimfinatfing the need for an externafl heater or optficafl fimage processfing scheme makes fit an findependent experfimentafl setup for finvestfigatfing phase-change heat transfer processes and usabfle wfithfin thermafl management hardware or

processfing equfipment.

4. Conclusions

Dropflet fimpact and subsequent evaporatfion of subcoofled fimpfingfing dropflets have been finvestfigated on a heated poflyfimfide surface at varyfing fimpact veflocfitfies and surface temperatures utfiflfizfing a custom MEMS devfice to determfine the underflyfing physfics behfind the phase-change heat transfer process. Thfis mficrodevfice facfiflfitated an findependent experfimentafl setup, ensurfing mficroscafle trackfing of the MCL vaflfidated by the temperature measurement of the RTDs. Experfimentafl resuflts have shown that when a dropflet fimpacts a heated surface and evaporates, the process can be dfivfided finto two segments based on the effectfive heat transfer rate: an fnfifiafl conductfion-domfinated segment foflflowed by another segment domfinated by surface evaporatfion. The experfimentafl finvestfigatfions have afso fled to the foflflowfing concflusfions:

- The ffirst segment, "sensfibfle heat regfime," corresponds to a sharp fincrease fin heat transfer rate upon dropflet fimpact, foflflowed by a graduafl decrease as heat fis befing conducted to the dropflet from the heated surface. In the second segment, the heat transfer assocfiated wfith mass transfer due to vapor removafl becomes domfinant and causes a nearfly constant heat transfer rate. Hfigher surface temperatures flengthen the sensfibfle heat regfime but shorten the constant heat transfer segment. The sensfibfle heat regfime exhfibfits hfigher heat transfer rates between these two segments.
- The effect of oscfiflflatory motfion fis negflfigfibfle for subcoofled fimpactfing dropflets, unflfike fin a superheated regfime; hence, heat conductfion finto the dropflet from the heated surface entfirefly domfinates the ffirst segment.
- Heat fflux caused by dropflet fimpact has a weaker dependence on surface temperature; conversefly, the recedfing MCL heat transfer fis sfignfifficantfly surface temperature dependent.
- The heat fflux at the soflfid–flfiqufid finterface of an fimpactfing dropflet fincreases wfith the rfise of efither fimpact veflocfity or surface temperature. The flocafl heat fflux vaflues due to dropflet fimpact are, on average, more than 12 tfimes hfigher than the fnfifiafl dry state and more than 4.5 tfimes hfigher than those assocfiated wfith the recedfing MCL movement. In the fffflm evaporatfion regfime, dropflets fimpactfing a heated surface have approxfimatefly 1.6 tfimes hfigher vertficafl heat fflux vaflues than gentfly deposfited dropflets.
- Buoyancy and thermocapfiflflary convectfion wfithfin evaporatfing dropflets contrfibute negflfigfibfly to overaflfl heat transfer, whfich fis domfinated by heat conductfion finto the dropflet and surface evaporatfion.

To summarfize, the experfimentafl resuflts of thfis work from studyfing the heat transfer regfimes and comprehendfing the transfitfion from conductfive heat transfer to surface evaporatfion durfing dropflet fimpfingement and foflflowfing evaporatfion can provfide essentfiafl finsfights finto underflyfing physfics to fimprove heat transfer modefls, surface engfineerfing, and overaflfl effectfiveness. Moreover, reafl-tfime, mfinfimaflfly finvasfive temperature measurements and sfimufltaneous trackfing of MCL at the mficroscafle by a composfite mficrodevfice utfiflfized fin thfis work can afid fin thermafl management and process controfl for eflectronfics cooflfing.

CRediT authorship contribution statement

Md Tanbin Hasan Mondal: Wrfitfing – orfigfinafl draft, Methodoflogy, Investfigatfion. **Md Shafayet Alam:** Wrfitfing – orfigfinafl draft. **Rifat-E-Nur Hossain:** Wrfitfing – orfigfinafl draft. **Arden L. Moore:** Wrfitfing – revfiew & edfitfing.

Declaration of competing interest

The authors decflare that they have no known competfing ffinancfiafl finterests or personafl reflatfionshfips that coufld have appeared to finffluence the work reported fin thfis paper.

Data availability

Data wfffl be made avafiflabfle on request.

Acknowledgements

Thfis materfiafl fis based upon work supported by the Natfionafl Scfience Foundatfion under Grant Number 1846165.

Appendix A. Supplementary data

Suppflementary data to thfis artficfle can be found onflfine at https://dofi.org/10.1016/j.appflthermafleng.2024.123152.

References

[1] G. Guggfiflfla, R. Narayanaswamy, A. Pattamatta, An experfimentafl finvestfigatfion finto the spread and heat transfer dynamfics of a trafin of two concentrfic fimpfingfing dropflets over a heated surface, Exp. Therm. Fflufid Scfi. 110 (September 2019) (2020) 109916.
[2] G. Lfiang, I. Mudawar, Revfiew of drop fimpact on heated waflfls, Int. J. Heat Mass Transf. 106 (2017) 103–126.
[3] J.D. Benther, J.D. Peflaez-Restrepo, C. Stanfley, G. Rosengarten, Heat transfer durfing mufltfipfle dropflet fimpfingement and spray cooflfing: revfiew and prospects for enhanced surfaces, Int. J. Heat Mass Transf. 178 (2021) 121587.
[4] S.L. Manzeflflo, J.C. Yang, An experfimentafl finvestfigatfion of water dropflet fimpfingement on a heated wax surface, Int. J. Heat Mass Transf. 47 (8–9) (2004) 1701–1709.
[5] S.L. Manzeflflo, J.C. Yang, An experfimentafl study of a water dropflet fimpfingfing on a flfiqufid surface, Exp. Fflufids 32 (5) (2002) 580–589.
[6] A. Ghoflfijanfi, C. Schflawfitschek, T. Gambaryan-Rofisman, P. Stephan, Heat transfer durfing drop fimpfingement onto a hot waflfl: the finffluence of waflfl superheat, fimpact veflocfity, and drop dfiameter, Int. J. Heat Mass Transf. 153 (2020) 119661.
[7] M. Pasandfideh-Fard, S.D. Azfiz, S. Chandra, J. Mostaghfimfi, Cooflfing effectfiveness of a water drop fimpfingfing on a hot surface, Int. J. Heat Fflufid Fflow 22 (2) (2001) 201–210.
[8] S. Herbert, S. Ffischer, T. Gambaryan-Rofisman, P. Stephan, Locafl heat transfer and phase change phenomena durfing sfingfle drop fimpfingement on a hot surface, Int. J. Heat Mass Transf. 61 (2013) 605–614.
[9] A. Ghoflfijanfi, T. Gambaryan-Rofisman, P. Stephan, Experfimentafl finvestfigatfion of hydrodynamfics and heat transport durfing vertficafl coaflescence of mufltfipfle successfive drops fimpactfing a hot waflfl under saturated vapor atmosphere, Exp. Therm. Fflufid Scfi. 118 (2020) 110145.
[10] P.K. Tyagfi, R. Kumar, P.K. Mondafl, A revfiew of the state-of-the-art nanofflufid spray and jet fimpfingement cooflfing, Phys. Fflufids 32 (12) (2020).
[11] S. Herbert, S. Ffischer, T. Gambaryan-Rofisman, P. Stephan, Locafl heat transfer and phase change phenomena durfing sfingfle drop fimpfingement on a hot surface, Int. J. Heat Mass Transf. 61 (1) (2013) 605–614.
[12] A.B. Wang, C.H. Lfin, C.C. Cheng, Pattern anaflysfis of a sfingfle dropflet fimpfingfing onto a heated pflate, Heat Transf. - Asfian Res. 34 (8) (2005) 579–594.
[13] S. Chandra, C.T. Avedfisfian, On the cofflfisfion of a dropflet wfith a soflfid surface, Proc. R. Soc. A Math. Phys. Eng. Scfi. 432 (1884) (1991) 13–41.
[14] H. Jones, M.H. Burden, G. Thursffiefld, H. Lfiu, E.J. Lavernfia, R.H. Rangefl, A rotary atomfizatfion technfique for bufk spflat cooflfing Spflat cooflfing and metastabfle phases H Jones A gas atomfizatfion spray quenchfing technfique for bufk spflat cooflfing Numerficafl sfimufiatfion of substrate fimpact and freezfing of dropflets fin pflasma spray processe, J. Phys. D Appfl. Phys 4 (1971) 1657.
[15] S. Moghtadernejad, C. Lee, M. Jadfidfi, An fintroductfion of dropflet fimpact dynamfics to engfineerfing students, Fflufids 5 (3) (2020) 1–18.
[16] A.R. Patfi, B. Swafin, S.S. Mohapatra, The bofiflfing phenomena and thefir proper fidentfiffication and dfiscrfimfinatfion methodoflogy, Scfi. Rep. 10 (1) (2020) 1–8.
[17] J.L. Pflawsky, et afl., Nano-and mficrostructures for thfin-ffiflm evaporatfion-a revfiew, Nanoscafle Mficroscafle Thermophys. Eng. 18 (3) (2014) 251–269.
[18] J.D. Bernardfin, C.J. Stebbfins, I. Mudawar, Mappfing of fimpact and heat transfer regfimes of water drops fimpfingfing on a poflfished surface, Int. J. Heat Mass Transf. 40 (2) (1997) 247–267.
[19] T. Tran, H.J.J. Staat, A. Prosperettfi, C. Sun, D. Lohse, Drop fimpact on superheated surfaces, Phys. Rev. Lett. 108 (3) (2012) 1–5.
[20] A.-B. Wang, C. Lfin, C.-C. Chen, The crfitficafl temperature of dry fimpact for tfiny dropflet fimpfingfing on a heated surface, Phys. Fflufids 12 (2000) 1622–1625.
[21] H.J.J. Staat, et afl., Phase dfiagram for dropflet fimpact on superheated surfaces, J. Fflufid Mech. 779 (2015) R3.
[22] S. Herbert, T. Gambaryan-Rofisman, P. Stephan, Inffluence of the governfing dfimensfionfless parameters on heat transfer durfing sfingfle drop fimpfingement onto a hot waflfl, Coflflofids Sur. A Physficochem. Eng. Asp. 432 (2013) 57–63.
[23] V.E. Nakoryakov, S.Y. Mfisyura, S.L. Eflfistratov, The behavfior of water dropflets on the heated surface, Int. J. Heat Mass Transf. 55 (23–24) (2012) 6609–6617.

[24] C. Qfiang, S. Chandra, S. McCahan, The effect of dfissoflvfing gases or soflfids fin water dropflets bofiflfing on a hot Surface, J. Heat Transfer 123 (4) (2001) 719–728.
[25] M.T.H. Mondafl, R.-E.-N. Hossafin, R. Martfin, A.L. Moore, Independent mficroscafle sensfing of phase finterface and surface temperature durfing dropflet evaporatfion, Appfl. Therm. Eng. 236 (2024) 121477.
[26] J. Lee, J. Kfim, K.T. Kfiger, Tfime- and space-resoflved heat transfer characterfistfics of sfingfle dropflet cooflfing usfing mficroscafle heater arrays, Int. J. Heat Pflufid Pflow 22 (2) (2001) 188–200.
[27] M.T.H. Mondafl, T. Desafi, R.-E.-N. Hossafin, A.L. Moore, Mficroscafle trackfing of unconstrafined movfing mufltfiphase contact flfines vfia a capacfitance sensor array, Sensors Actuators A Phys. 331 (2021) 113046.
[28] M.T.H. Mondafl, R.-E.-N. Hossafin, R. Martfin, A.L. Moore, Speed and flocatfion trackfing of movfing mufltfiphase finterfaces vfia a capacfitance mficrosensor array durfing dropflet evaporatfion, Mficro Nano Eng. (2022) 100168.
[29] W. Huang, et afl., Dropflet evaporatfion on hot mficro-structured superhydrophobfic Surfaces: anaflysfis of evaporatfion from dropflet cap and base Surfaces, Int. J. Heat Mass Transf. 185 (2022).
[30] R. Hays, D. Maynes, J. Crockett, Thermafl transport to dropflets on heated superhydrophobfic substrates, Int. J. Heat Mass Transf. 98 (2016) 70–80.
[31] D. Zang, S. Tarafdar, Y.Y. Tarasevfich, M. Dutta Choudhury, T. Dutta, Evaporatfion of a dropflet: from physfics to appflficatfions, Phys. Rep. 804 (2019) 1–56.
[32] G. Lu, Y.Y. Duan, X.D. Wang, D.J. Lee, Internafl fflow fin evaporatfing dropflet on heated soflfid surface, Int. J. Heat Mass Transf. 54 (19–20) (2011) 4437–4447.
[33] A. Chandramohan, S. Dash, J.A. Wefibefl, X. Chen, S.V. Garfimeflfla, Marangonfi convectfion fin evaporatfing organfic flfiqufid dropflets on a nonwettfing substrate, Langmufir 32 (19) (2016) 4729–4735.